PRECLINICAL VALIDATION OF TARGET ENGAGEMENT ASSAYS AND INVESTIGATION OF MECHANISTIC IMPACTS OF FHD-609, A CLINICAL-STAGE BRD9 DEGRADER BEING DEVELOPED FOR THE TREATMENT OF SYNOVIAL SARCOMA

Mike Collins, Jessica Wan, Victoria Garbitt-Amaral, Brandon Antonakos, Hsin-Jung Wu, Christina Xu, David L. Lahr, Liyue Huang, Virna Schuck, Qianhe Zhou, Ammar Adam, Ray Chen, Scott Innis, Samuel Agresta and Jessica Piel

Foghorn Therapeutics, 500 Technology Square, Cambridge, MA 02139

FOGHORN® THERAPEUTICS

Abstract

Synovial sarcomas express the SSX-SS18 fusion oncoprotein, which drives tumorigenesis by compromising the function of the BAF (BRG/BRM-associated factors) chromatin remodeling complex. Cells with this form of BAF perturbation are heavily dependent on the non-canonical BAF (ncBAF) subunit BRD9 (Bromodomain-containing protein 9) for survival. However, the mechanism by which BRD9 promotes tumor growth is not well understood.

FHD-609 is a heterobifunctional degrader of BRD9 that is currently in clinical development for the treatment of advanced synovial sarcoma. Assays to measure the abundance of BRD9 protein in patient tumors will be important for demonstrating target engagement with FHD-609. Additionally, because tumor biopsies occur infrequently, assays to monitor BRD9 levels in peripheral tissues may permit longitudinal analysis of BRD9 degradation in patients treated with FHD-609. The objectives of the present study were to develop clinically relevant assays to quantify BRD9 protein levels in tumor and peripheral blood mononuclear cells (PBMCs), to profile the pharmacodynamics (PD) of FHD-609 in these tissues, and to explore the downstream impacts of BRD9 degradation in synovial sarcoma.

Background

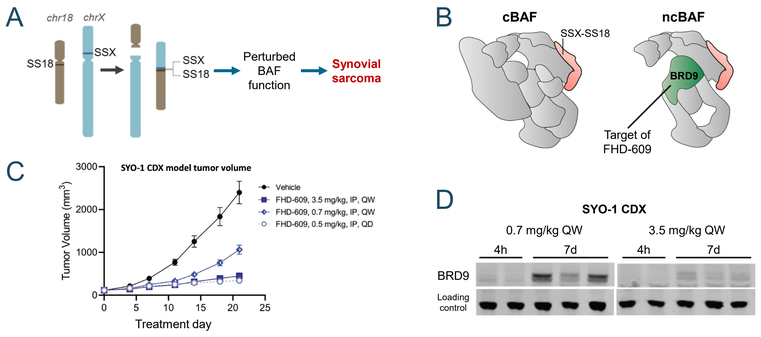

Figure 1. A) Illustration of the SSX-SS18 translocation, the defining genetic hallmark of synovial sarcoma. **B)** Composition of cBAF and ncBAF complexes. SSX-SS18 perturbs normal cBAF functionality and renders cells dependent upon ncBAF for survival. BRD9 is a unique subunit of ncBAF and the target of FHD-609. **C)** FHD-609 demonstrates dose-dependent tumor growth inhibition in cell line-derived xenograft (CDX) models of synovial sarcoma. IP = intraperitoneal; QW = weekly dosing; QD = daily dosing. **D)** BRD9 levels assessed by western blot in tumor lysates collected at indicated timepoints post last dose. Complete degradation between doses is required for maximal antitumor efficacy.

Methods

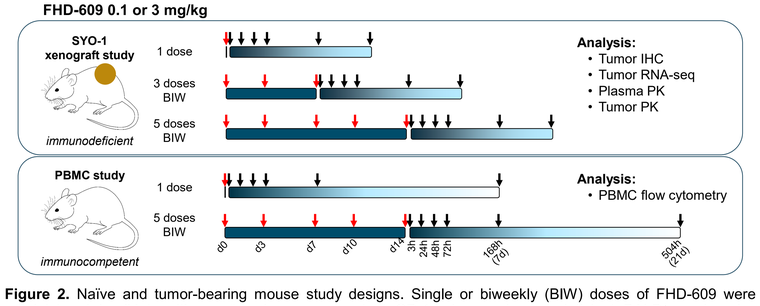

Figure 2. Naïve and tumor-bearing mouse study designs. Single or biweekly (BIW) doses of FHD-609 were administered by IV to either naïve, immunocompetent CD-1 mice, or immunodeficient BALB/c nude mice implanted with SYO-1 xenografts. Timepoints for analysis refer to collection time following the last dose. Red arrows indicate doses, and blue arrows indicate sample collections.

References and Acknowledgements

Kadoch, C. and Crabtree, G. R. (2013) Reversible disruption of mSWI/SNF (BAF) complexes by the SS18-SSX oncogenic fusion in synovial sarcoma. *Cell*. **153**, 71–85

Michel, B. C., *et al.* (2018) A non-canonical SWI/SNF complex is a synthetic lethal target in cancers driven by BAF complex perturbation. *Nat. Cell Biol.* **20**, 1410–1420

Centore, R. C., *et al.* (2020) Mammalian SWI/SNF chromatin remodeling complexes: Emerging mechanisms and therapeutic strategies. *Trends Genet.* **36**, 936–950

We wish to thank the patients, clinicians and investigators for their participation in the Phase 1 clinical trial of FHD-609

Novel IHC method to quantify BRD9 degradation in tumor tissue caused by *in vivo* FHD-609 treatment

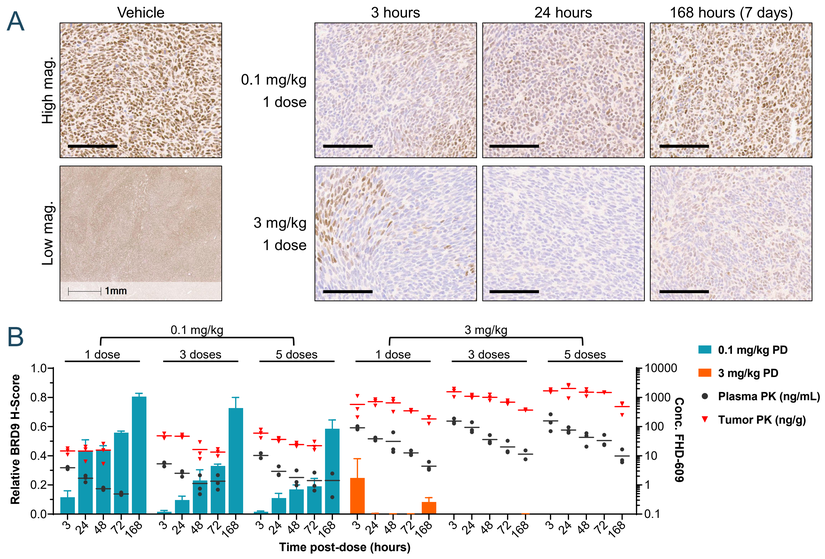

Figure 3. A) Mice bearing SYO-1 xenografts were treated with vehicle or FHD-609 at the doses and schedules shown in Fig. 2, and tumors were collected for analysis at the indicated timepoints. Shown are representative images of BRD9 protein detected by immunohistochemistry (IHC). Scale bars = 100 µm unless otherwise indicated. **B)** BRD9 IHC was quantified on a per-cell basis by image analysis using HALO v3.3 (Indica Labs) and scored according to the formula H-score = (1 × $\%_{weak}$) + (2 × $\%_{medium}$) + (1 × $\%_{strong}$). Bars represent mean H-score normalized to vehicle control and error bars are SEM. Concentrations of FHD-609 were measured in plasma and tumors from the same mice used for IHC analysis. Symbols represent individual animal values, and lines represent group means. Absence of symbols indicates values below LLOQ. *n* = 3 for all groups.

Novel flow cytometry method to quantify BRD9 degradation in PBMCs caused by *in vivo* FHD-609 treatment

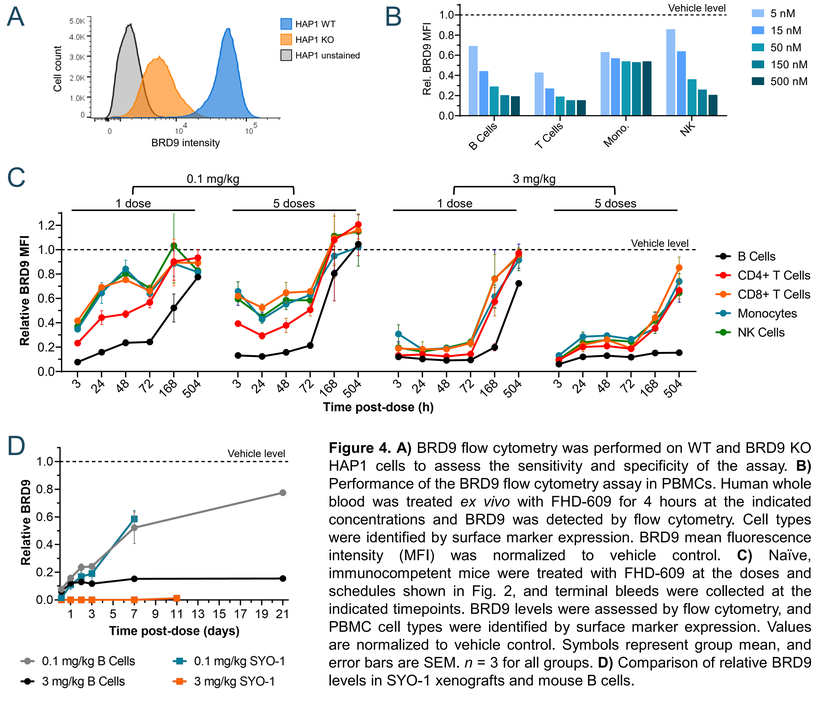

Figure 4. A) BRD9 flow cytometry was performed on WT and BRD9 KO HAP1 cells to assess the sensitivity and specificity of the assay. **B)** Performance of the BRD9 flow cytometry assay in PBMCs. Human whole blood was treated *ex vivo* with FHD-609 for 4 hours at the indicated concentrations and BRD9 was detected by flow cytometry. Cell types were identified by surface marker expression. BRD9 mean fluorescence intensity (MFI) was normalized to vehicle control. **C)** Naïve, immunocompetent mice were treated with FHD-609 at the doses and schedules shown in Fig. 2, and terminal bleeds were collected at the indicated timepoints. BRD9 levels were assessed by flow cytometry, and PBMC cell types were identified by surface marker expression. Values are normalized to vehicle control. Symbols represent group mean, and error bars are SEM. *n* = 3 for all groups. **D)** Comparison of relative BRD9 levels in SYO-1 xenografts and mouse B cells.

FHD-609 treatment decreases Myc expression and gene sets, and decreases markers of proliferation in tumors *in vivo*

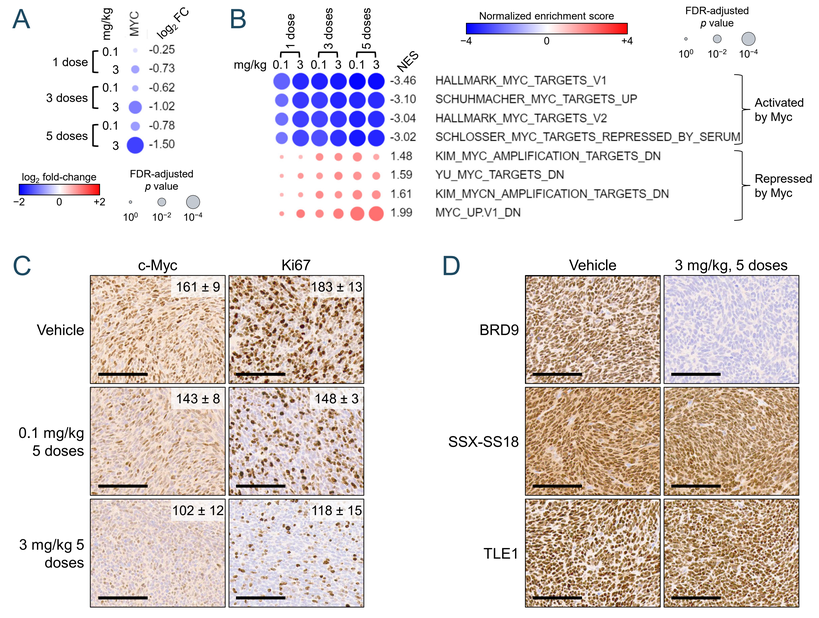

Figure 5. A) Differential gene expression (DGE) of *MYC* measured by RNA sequencing (RNA-seq) in SYO-1 xenografts 24 hours after treatment with vehicle or FHD-609. DGE is expressed as $\log_2$ fold-change relative to vehicle. Circles are sized by statistical significance. **B)** Gene set enrichment analysis (GSEA) following RNA-seq of SYO-1 xenografts 24 hours after treatment with vehicle or FHD-609. Selected upregulated and downregulated gene sets, and the average normalized enrichment scores (NES) across treatment groups, are shown. Out of 21,688 gene sets analyzed, HALLMARK_MYC_TARGETS_V1 is the top gene set by average negative NES. Circles are colored by NES and sized by statistical significance. **C)** Representative images of c-Myc and Ki67 detected by IHC in SYO-1 xenografts from mice treated with vehicle or FHD-609 at the indicated doses and timepoints. Scale bars = 100 µM. Values are H-scores, as quantified by image analysis. **D)** Representative IHC images showing no change in SSX-SS18 and TLE1 expression in SYO-1 xenografts treated with FHD-609 at 3 mg/kg for 5 doses. BRD9 levels in these same tumors are shown for reference of target engagement. Scale bars = 100 µm.

Early analysis of patient tumor biopsies shows BRD9 degradation following FHD-609 treatment

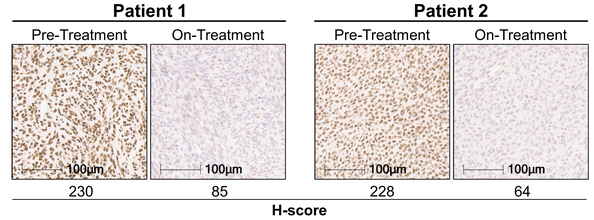

Figure 6. Representative BRD9 IHC images of tumor biopsies from two patients with metastatic synovial sarcoma treated with the same low dose of FHD-609. Biopsies were taken either 2 days (Patient 1) or 1 day (Patient 2) following FHD-609 administration. H-scores were generated by a board-certified pathologist.

Conclusions

- Newly validated IHC and flow cytometry assays demonstrate excellent sensitivity and specificity for BRD9 in tumor tissue and PBMCs, respectively
- Target degradation in tumors is rapid and robust, but complete degradation is required between doses for maximal efficacy
- PBMCs are an effective surrogate for target engagement in tumors
- FHD-609 treatment decreases Myc expression and related gene sets, and decreases markers of proliferation in tumors *in vivo*
- BRD9 IHC and flow cytometry assays are being used to assess the pharmacodynamics of FHD-609 in a Phase I study in synovial sarcoma
- BRD9 degradation demonstrated in patient tumor biopsies